Cell

Identification of a Lipokine, a Lipid Hormone Linking Adipose Tissue to Systemic Metabolism

Haiming Cao,[1] Kristin Gerhold,[1,3] Jared R. Mayers,[1] Michelle M. Wiest,[2] Steven M. Watkins,[2] and Gökhan S. Hotamisligil[1,*]
[1]Department of Genetics and Complex Diseases, Harvard School of Public Health, Boston, MA 02115, USA
[2]Lipomics Technologies, West Sacramento, CA 95691, USA
[3]Present addresses: Department of Molecular and Cell Biology, University of California, Berkeley, Berkeley, CA 94703, USA
*Correspondence: ghotamis@hsph.harvard.edu
DOI 10.1016/j.cell.2008.07.048

SUMMARY

Dysregulation of lipid metabolism in individual tissues leads to systemic disruption of insulin action and glucose metabolism. Utilizing quantitative lipidomic analyses and mice deficient in adipose tissue lipid chaperones aP2 and mal1, we explored how metabolic alterations in adipose tissue are linked to whole-body metabolism through lipid signals. A robust increase in de novo lipogenesis rendered the adipose tissue of these mice resistant to the deleterious effects of dietary lipid exposure. Systemic lipid profiling also led to identification of C16:1n7-palmitoleate as an adipose tissue-derived lipid hormone that strongly stimulates muscle insulin action and suppresses hepatosteatosis. Our data reveal a lipid-mediated endocrine network and demonstrate that adipose tissue uses lipokines such as C16:1n7-palmitoleate to communicate with distant organs and regulate systemic metabolic homeostasis.

INTRODUCTION

In recent years, the world has seen an alarming increase in obesity and related metabolic diseases such as diabetes, fatty liver disease, and atherosclerosis that often form a disease cluster referred to as metabolic syndrome (Eckel et al., 2005). Dysregulation of lipid metabolism has been identified as a critical contributor to the mechanistic link between these pathologies (Ginsberg et al., 2006). For example, increased release of free fatty acids (FFAs) from adipose tissue has long been linked to muscle insulin resistance (Bergman and Ader, 2000) and lipogenesis and steatosis in liver (Ginsberg et al., 2006). The imbalance between liver-derived very-low-density lipoprotein (VLDL) and high-density lipoprotein (HDL) is a critical risk factor for the development of atherosclerosis and has also been linked to insulin resistance at peripheral tissues (Avramoglu et al., 2006). Epidemiological and clinical studies indicate that dietary lipids affect and sometimes even determine the course of development of metabolic syndrome (Warensjo et al., 2005). Despite a growing body of evidence supporting the key role lipid metabolism plays in metabolic diseases, the underlying mechanistic details by which alterations in tissue-specific lipid metabolism are directly integrated into systemic metabolic homeostasis are not well understood.

Many lipid species interact with fatty acid-binding proteins (FABPs), lipid chaperones that dictate the partitioning of lipids inside cells. Several FABPs have been reported to play critical roles in systemic metabolism (Furuhashi and Hotamisligil, 2008). Mice deficient in the major adipose FABP (aP2) have improved insulin sensitivity (Hotamisligil et al., 1996). The combined deficiency of aP2 and mal1 (FABP4 and FABP5, respectively) has a profound impact on systemic metabolic regulation and renders mice resistant to almost all components of metabolic syndrome (Maeda et al., 2005). Liver FABP-deficient mice gain less weight and have reduced hepatic steatosis (Newberry et al., 2006). Moreover, FABP expression is often altered in metabolic diseases such as atherosclerosis, type 2 diabetes, and obesity. This also applies to human disease where a genetic variation at the aP2 locus has been linked to cardiovascular disease and diabetes (Tuncman et al., 2006). The critical role of FABPs in metabolic diseases was highlighted by the recent demonstration that an orally active aP2 inhibitor could ameliorate metabolic syndrome in mice (Furuhashi et al., 2007). Since expression of most FABPs is highly tissue-specific, it is generally assumed that genetic manipulation would lead to alterations in lipid profiles, metabolic responses, or other functions restricted to those sites. In practice, however, changes resulting from FABP deficiency, especially adipose tissue FABPs (4 and 5), are often systemic, indicating that these molecules represent part of an endocrine pathway(s) that organisms have evolved to maintain overall metabolic balance. Hence, genetic loss-of-function models of cytosolic lipid chaperones constitute powerful experimental systems for the exploration of unique aspects of lipid metabolism and signaling both inside cells and between organs.

In this study, we utilized adipose tissue lipid chaperones to explore lipid-based pathways and signals by which local alterations in adipose tissue are connected to systemic metabolic outcomes. Utilizing high-density, quantitative lipidomic analysis, as well as physiological and molecular approaches in FABP-deficient models, we provided evidence that the impact of adipose tissue on the specific composition of local

and circulating FFAs is critical in determining metabolic outcomes. We then identified a specific lipid hormone or a "lipokine" responsible for linking adipose tissue to systemic metabolism.

RESULTS

Impact of Lipid Chaperones on Systemic Lipid Distribution and Composition

We have previously observed significant changes of major lipid clusters in aP2-mal1$^{-/-}$ (FABP-deficient, FABP$^{-/-}$) mice, raising the possibility that circulating lipids might regulate systemic metabolic responses in this model (Maeda et al., 2005). To explore the role of FABP-regulated lipid signaling networks in metabolic homeostasis, we performed high-resolution lipidomics analyses that allow for accurate quantification of over 400 lipid species in a single sample.

We analyzed plasma and all major insulin-responsive tissues from WT and FABP$^{-/-}$ mice kept on either regular or high-fat diet (HFD). To capture all FABP-deficiency- or diet-driven alterations in lipid profile, we first performed unsupervised cluster analyses focusing on all lipid species that exhibit statistical differences. Tissue samples from individual WT or FABP$^{-/-}$ mice under the same diet segregated into tight clusters (Figure 1A), indicating that the lipid chaperones have profound effects on systemic lipid metabolism and that their absence in adipose tissue caused identifiable global changes in tissue lipid profiles. Moreover, plasma, liver, and muscle tissues of mice on either diet fell into distinctly separated clusters irrespective of genotype (Figure 1A), indicating that dietary lipids have greater effects than genotype on lipid composition and metabolism in these tissues. This is not unexpected, since dietary intake is a major factor that determines tissue lipid composition (Field and Clandinin, 1984). Surprisingly, however, adipose tissues of FABP$^{-/-}$ mice under HFD clustered with both genotypes on regular diet (Figure 1A), indicating that specifically in adipose tissue, FABP deficiency has greater effects on lipid composition than does diet. Indeed, the adipose tissue of these mice maintained a lipid profile reminiscent of lean, insulin-sensitive WT controls despite exposure to HFD and dramatically differed from that of obese and insulin-resistant WT animals.

Next, we used two additional approaches to further explore the impact of lipid chaperones on tissue responsiveness to diet. First, we performed principal component analysis (PCA) to reveal the main factors underlying the structure of the local and systemic lipid profiles (Figure 1B). For plasma, liver, and muscle, the first two principal components effectively separated the animals into four distinct groups, the first principal component separating diets (x axis) and the second separating genotypes (y axis). For adipose tissue, however, the data points representing FABP$^{-/-}$ mice on both diets were essentially overlapping, indicating that the dietary effects at this site are significantly less pronounced. Next, we calculated the strength of the impact of diet on each tissue and expressed the ranked p values against each other (Figure 1C). This analysis did not identify differences between genotypes in muscle. In contrast, adipose tissue of FABP$^{-/-}$ mice had substantially fewer lipid species that were regulated by diet than did that of the WT. These observations support the argument that unlike other tissues, HFD fails to cause a significant change in the overall lipid profile of adipose tissue in FABP$^{-/-}$ mice. A similar property was also detected upon examination of the triglyceride (TG) component, which was dissociated from dietary intake specifically in adipose tissue of FABP$^{-/-}$ mice (Figure S1 available online).

These results clearly demonstrate that lipid chaperones are required intermediaries between dietary input and adipose tissue lipids. This is an unprecedented and remarkable result, given that even the mutation of genes directly involved in lipid metabolism can rarely render tissue lipid profiles resistant to dietary effects.

Enhanced De Novo Lipogenesis in Adipose Tissue Leads to Dramatically Increased Plasma C16:1n7-Palmitoleate

Since adipose tissue of FABP$^{-/-}$ mice is resistant to diet-induced insulin resistance, the unique lipid profile observed in these mice suggests a direct link between lipid metabolism and composition and the improved metabolic responses in these animals. Therefore, we examined the lipid profile of this tissue in detail. We observed a striking enrichment of one particular fatty acid, C16:1n7-palmitoleate (Figure 2A), in all major lipid classes analyzed in adipose tissues of FABP$^{-/-}$ mice. In fact, palmitoleate was by far the most significantly regulated lipid species in adipose tissue (Figure 2B). Adipose tissue is the major source of circulating FFAs, and alterations in adipose lipid metabolism are often reflected in plasma FFAs. Systematic comparison of plasma FFAs in FABP$^{-/-}$ versus WT mice identified palmitoleate as the top ranking species among all regulated lipids (Figure S2). Plasma palmitoleate concentration was increased in FABP$^{-/-}$ mice under both regular and high-fat diets, and the magnitude of the absolute quantitative increase was very substantial, rendering palmitoleate as the third most abundant FFA in the plasma of FABP$^{-/-}$ animals (Figure 2C and Figure S3). Analysis of other essential lipid species both in individual tissues and systemically (Figures S4–S6) did not identify any major changes. These observations led us to investigate the possibility that increased adipose and serum palmitoleate might be a key change in lipid metabolism that underlies the improved systemic energy homeostasis in FABP$^{-/-}$ mice. Total palmitoleate in the adipose tissue of WT mice was reduced by nearly 50% upon exposure to HFD, but FABP$^{-/-}$ animals experienced only 10% reduction, demonstrating that FABP-deficiency produces marked resistance to dietary regulation of palmitoleate in adipose tissue (Figure 2D). Using post hoc comparisons of our lipidomic analysis, we found that there was a dramatic decrease of palmitoleate in adipose triglyceride of WT mice on HFD compared to controls on regular diet (Figure S7). In contrast, there was no difference in palmitoleate between FABP$^{-/-}$ mice on either diet. This resistance to dietary suppression of palmitoleate was also reflected in plasma (Figure S3). In short, increased palmitoleate in adipose tissue and plasma is the most significant change in overall lipid metabolism in FABP$^{-/-}$ mice.

Palmitoleate is a unique fatty acid that serves as a marker for de novo lipogenesis, a process that converts glucose to fatty acids. The levels of palmitoleate in the diet are low, and

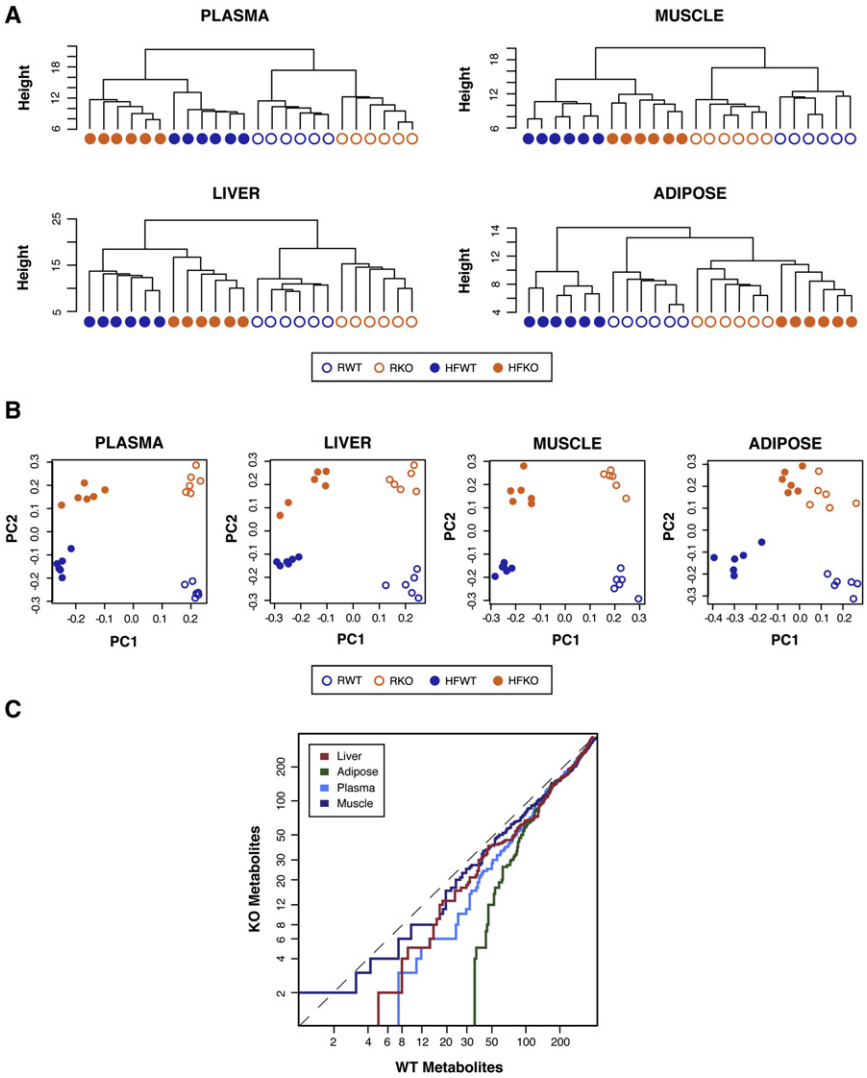


Figure 1. Whole-Body Lipid Profiling

(A) Dendrograms of hierarchical clustering of subjects, based on lipid profiles. Only fatty acids with a p value < 0.05 from a one-way ANOVA were included. R, regular diet; HF, high-fat diet; KO, FABP$^{-/-}$ mice.

(B) Scatter plots of principal components from principal component analysis on subjects. Only fatty acids with a p value < 0.05 from a one-way ANOVA were included.

(C) Strength of differences between diets in the WT and FABP$^{-/-}$ (KO) mice over all fatty acids in all lipid classes. Each point on a line indicates the number of p values of one group that are smaller than the p value of equal ranking of the other group.

consequently its concentration in tissues is minimal, although concentrations can quickly and substantially increase upon activation of de novo lipogenesis. The pattern we observed suggested a potential regulatory role for lipid chaperones in the production of this lipid signal and warranted an investigation of palmitoleate's mechanism of action and effects on biological outcomes.

Contribution of C16:1n7-Palmitoleate in Plasma Lipids to Metabolic Regulation

Increased circulating FFAs in obesity have been linked to peripheral insulin resistance and enhanced lipid synthesis and accumulation in liver. Paradoxically, however, FABP$^{-/-}$ mice have significantly higher total plasma FFAs than do WT controls and yet maintain superior insulin sensitivity and are completely protected from fatty liver disease (Maeda et al., 2005). Neither adiponectin nor leptin plays a significant role in this metabolic profile (Cao et al., 2006), indicating that palmitoleate might be a hormonal signal emerging from adipose tissue to improve systemic metabolic outcomes in FABP$^{-/-}$ mice.

To examine this possibility, we developed several highly sensitive assays to probe the functional profile and activities of plasma lipids. We chose SCD-1 as a readout because hepatic SCD-1 activity is suppressed in FABP$^{-/-}$ mice under diet-induced or genetic obesity (Cao et al., 2006; Maeda et al., 2005). Hepatic SCD-1 expression is regulated by a variety of hormones and nutritional factors including insulin and polyunsaturated fatty acids (PUFAs) (Ntambi and Miyazaki, 2004) via transcription factor-binding elements located 1.5 kb upstream of the SCD-1 transcription initiation site (Chu et al., 2006; Ntambi, 1999). We cloned this promoter region in front of luciferase gene and produced a reporter adenovirus. FAO rat hepatoma cells infected with this adenovirus were responsive to PUFAs, consistent with previous observations (Figure S8). We then adapted this assay system to a microplate format, sensitive to small amounts of lipids, which allowed us to test the effects of lipids extracted from plasma of WT and FABP$^{-/-}$ animals.

Although SCD-1 promoter activity in liver cells treated with lipids from WT plasma showed little difference from that in nontreated cells, the reporter activity in cells treated with lipids extracted from FABP$^{-/-}$ plasma was reduced by 40% (Figure 3A). These results indicate that plasma lipids from FABP$^{-/-}$ mice carry an activity that suppresses SCD-1 expression in liver cells. To distinguish between differences in the total lipid amount versus lipid composition, we generated mixtures of FFAs with the same molar ratios detected in WT or FABP$^{-/-}$ plasma lipids using the major fatty acids listed in Figure 2C. Interestingly, these lipid mixtures exerted the same pattern of activity as their corresponding plasma composition (Figure 3B). When the high concentration of palmitoleate in the lipid mixture mimicking the plasma of FABP$^{-/-}$ mice was reduced to the level seen in WT mice without other lipid components or total content

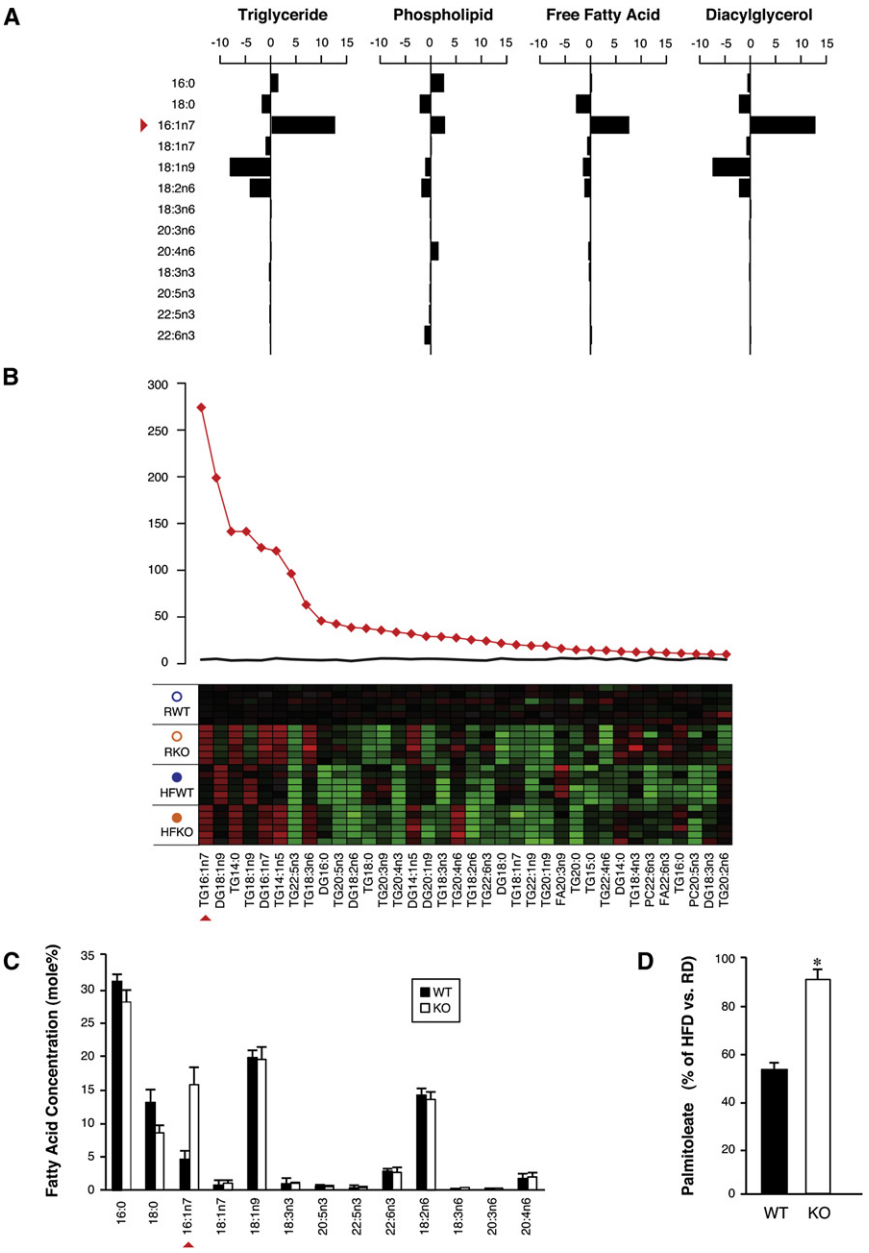


Figure 2. Adipose De Novo Lipogenesis and Palmitoleate Production

(A) Difference of major fatty acids in diacylglycerol, free fatty acid, phospholipid, and triglyceride fractions in adipose tissue between the means of WT and FABP$^{-/-}$ mice.

(B) Lipid class composition analysis for fatty acids in adipose tissue. The top 36 metabolites are shown. The F statistics from a one-way ANOVA are displayed as red diamonds over the distribution of F statistics from permuted data. The black line is the maximum F statistic observed in 100 permutations. The heat map displays the observed data, centered to the mean of the control group and scaled by the standard deviation of all observations.

(C) Plasma fatty acids in WT or FABP$^{-/-}$ (KO) mice.

(D) Percentile suppression of palmitoleate by HFD in adipose tissue of WT or KO mice.

Error bars represent the SEM.

being changed, the SCD-1-suppressing activity was significantly diminished (Figure 3B). These results demonstrate that palmitoleate is the main lipid component contributing to the regulation of SCD-1 expression. Plasma of FABP$^{-/-}$ mice also exhibits slightly reduced palmitate and stearate (Figure 2C), which might explain the residual activity retained in lipid mixture mimicking FABP deficiency after the reduction of palmitoleate. Indeed, after adjustment of these two lipid quantities in FABP$^{-/-}$ lipid mixture to WT levels, the SCD-1-suppressing activity was completely lost (Figure 3B).

Previously, we have also observed significantly improved whole-body glucose disposal and increased muscle glucose uptake in FABP$^{-/-}$ mice. To investigate whether plasma lipids play a role in regulating muscle insulin action, we treated differentiated C2C12 myotubes with lipid extracts and determined insulin-stimulated AKT phosphorylation using an ELISA system. We found that myotubes pretreated with plasma lipids extracted from FABP$^{-/-}$ mice had significantly enhanced AKT phosphorylation upon insulin treatment compared to those exposed to WT lipids (Figure 3C). Similar results were also observed by immunoblotting analysis (Figure 3C, inset). These results indicated that the unique plasma lipid profile of FABP$^{-/-}$ mice may also play a role in the insulin-sensitizing effect of FABP deficiency on muscle tissue.

Obesity is associated with low-grade inflammation in liver and adipose tissues, which contributes to the development of systemic insulin resistance (Hotamisligil, 2006). To explore the effect of plasma lipids on inflammatory responses, we treated explants of adipose tissue with lipids from WT or FABP$^{-/-}$ mice. MCP-1 secretion from adipose explants treated with WT lipids was significantly higher than those treated with FABP$^{-/-}$ lipids (Figure 3D), suggesting that these lipids also regulate adipose tissue inflammatory output. Since adipose tissue contains multiple cell populations in addition to fat cells, we separated adipose tissue into adipocytes and stromal vascular fractions and treated each fraction with either palmitate or palmitoleate. Interestingly, palmitoleate suppressed cytokine expression in adipocyte fractions as compared to palmitate, but the two lipids have similar effects on stromal vascular cells (Figure S9). These results indicate that adipocytes are the major targets for bioactive lipids.

Our observations to this point raise the possibility that palmitoleate is the lipid species responsible, at least in part, for the metabolic activities linked to adipose tissue FABPs. To investigate

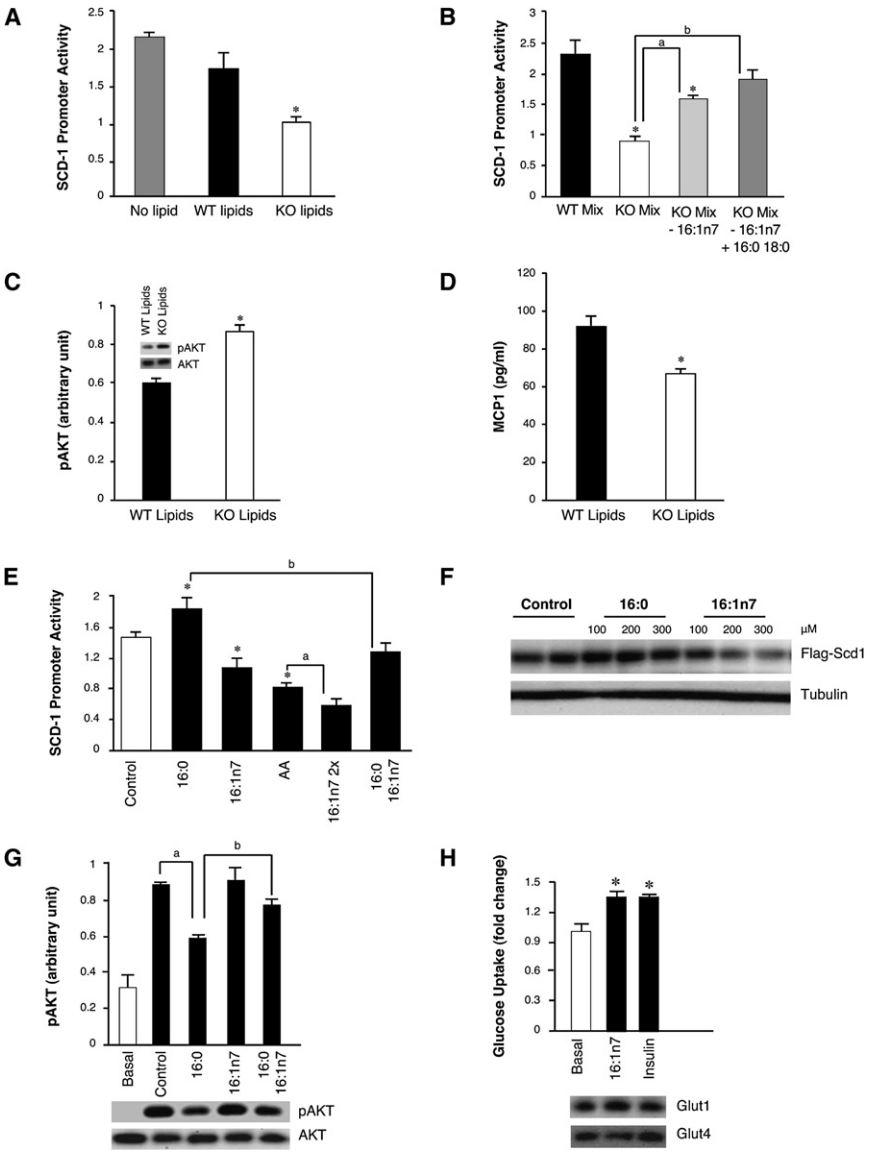


Figure 3. Metabolic Regulation by Plasma Lipids

(A) SCD-1 promoter activities in control hepatocytes (No lipid) or hepatocytes treated with plasma lipids extracted from WT or FABP$^{-/-}$ (KO) mice.

(B) SCD-1 promoter activities in hepatocytes treated with fatty acid mixtures resembling the ratio of plasma fatty acids from WT mice (WT Mix), KO mice (KO Mix), KO mice with the concentration of palmitoleate of WT mice (KO Mix, − 16:1n7), or KO mice with the concentration of palmitoleate, palmitate, and stearate of WT mice (KO Mix, − 16:1n7, + 16:0 18:0). Asterisk, significantly different from WT mix; a and b, significantly different from KO Mix.

(C) Insulin-stimulated AKT phosphorylation in C2C12 myotubes treated with plasma lipids extracted from WT or KO mice. Values of bar plot were determined by phospho-AKT ELISA, and corresponding immunoblotting results are shown as insets.

(D) MCP1 in conditional medium of adipose explants treated with plasma lipids of WT or KO mice.

(E) SCD-1 promoter activities in hepatocytes treated with fatty acids. All fatty acids were used at 300 μM final concentration, except 16:1n7 2x is 600 μM. AA, arachidonic acid; asterisk, significantly different from controls; a, significantly different from AA-treated cells; b, significantly different from palmitate-treated cells.

(F) Immunobloting of Flag-tagged SCD-1 in hepatocytes treated with control, palmitate, and palmitoleate. Tubulin was used as loading control.

(G) AKT phosphorylation in C2C12 myotubes treated with fatty acids and insulin. a, significantly different from cells treated with insulin; b, significantly different from cells treated with both insulin and palmitate. The bottom panel shows the corresponding immunoblotting of total and phosphorylated AKT in cells treated with pooled lipids.

(H) Glucose uptake in C2C12 myotubes treated with insulin or palmitoleate. The bottom panel is immunoblotting of C2C12 cell lysates treated with insulin or palmitoleate with anti-Glut1 or Glut4 antibodies. Asterisk, $p < 0.05$.

Error bars represent the SEM.

this, we treated liver cells expressing the SCD-1 promoter reporter with palmitoleate and several other lipids. In this setting, palmitate increased SCD-1 promoter activity, whereas palmitoleate suppressed it (Figure 3E). Interestingly, palmitoleate also antagonized the effect of palmitate on SCD-1 promoter activity when cells were treated with a mixture of the two lipids. The suppressive impact of palmitoleate on SCD-1 promoter activity was comparable to arachidonic acid (AA), the well-established lipid mediator known to suppress SCD-1 expression. Since palmitoleate is nearly ten times more abundant in the plasma of FABP$^{-/-}$ mice than AA (Figure 2C), it is more likely to account for the regulation of SCD-1 under physiologically relevant conditions. We also examined the effects of palmitoleate on SCD-1 protein, which is known to have a very short half-life (Heinemann and Ozols, 2003), by expressing a Flag-tagged SCD-1 under the cytomegalovirus (CMV) promoter. Whereas palmitate stabilized SCD-1, palmitoleate significantly increased SCD-1 protein degradation (Figure 3F). This observation suggests that palmitoleate regulates SCD-1 abundance via several parallel mechanisms, which may collectively cause the dramatic suppression of liver SCD-1 activity in FABP$^{-/-}$ mice (Maeda et al., 2005).

To explore the effect of palmitoleate on muscle insulin signaling, we pretreated C2C12 myotubes with either palmitate or palmitoleate and then stimulated with insulin. Palmitate significantly reduced insulin-stimulated AKT phosphorylation, whereas palmitoleate has little effect on its own (Figure 3G). When cells were cotreated with both lipids, however, palmitoleate rescued the palmitate-induced reduction in insulin-stimulated AKT phosphorylation. Moreover, palmitoleate itself stimulated glucose uptake into C2C12 cells to a level similar to insulin (Figure 3H). The mechanism of this increase is not known and is not associated with alterations in the levels of Glut1 and Glut4 proteins (Figure 3H).

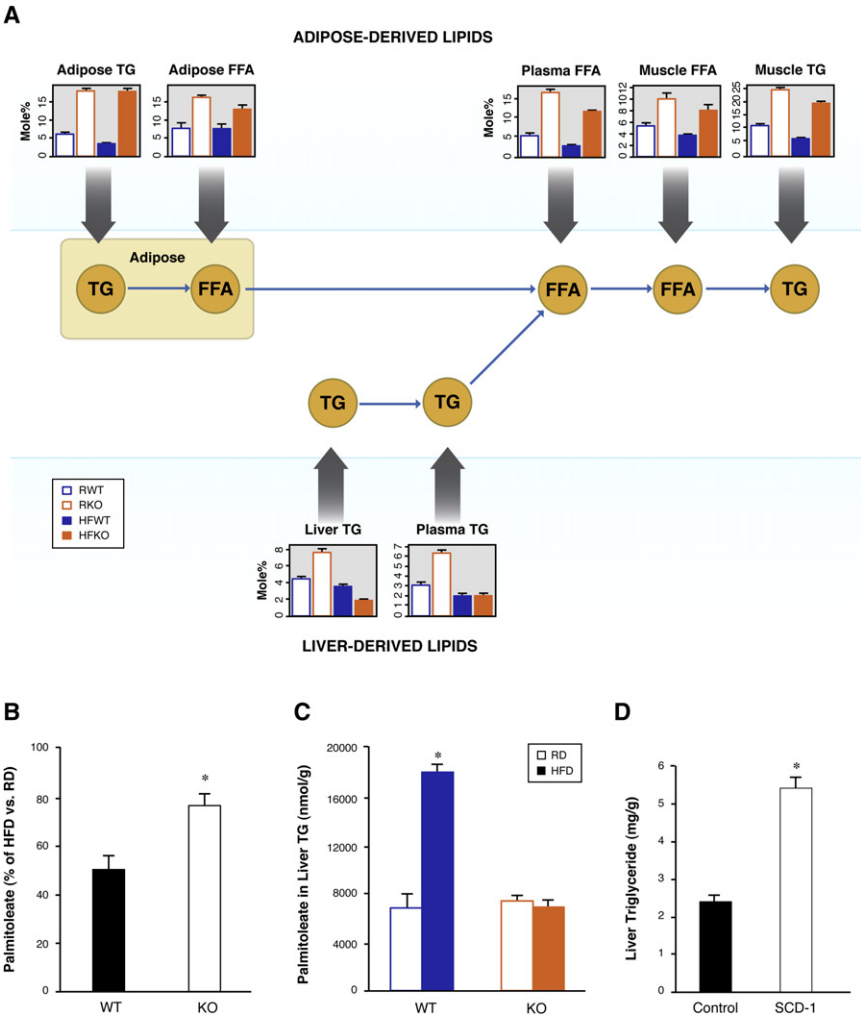


Figure 4. Systemic Palmitoleate Metabolism

(A) Free fatty acid and triglyceride flux among adipose, muscle, and liver tissues. Means and SEM of palmitoleate in free fatty acids (FFA) and triglyceride (TG) in plasma and adipose, muscle, and liver tissues of WT and FABP$^{-/-}$ mice are shown. The predicted lipid flux based on the tissue lipid profile pattern is indicated by the direction of arrows. Muscle fatty acids are mainly derived from liver in the form of VLDL-associated TG and from adipose tissue in the form of FFAs.

(B) Percentile suppression of palmitoleate by HFD in TG fraction of muscle tissue in WT or KO mice.

(C) Total palmitoleate in liver of WT or KO mice.

(D) Triglycerides in liver of KO mice injected with control or SCD-1 adenoviruses. Asterisk, $p < 0.05$. Error bars represent the SEM.

Whole-Body Metabolism of Palmitoleate Supports Its Role in Systemic Metabolic Regulation

To investigate tissue-specific effects of palmitoleate in metabolic homeostasis, we first examined metabolism of palmitoleate in muscle and liver in relation to adipose tissue by utilizing lipidomic and informatic tools. The supply of fatty acids to muscle is comprised mainly of FFAs derived from adipose tissue and fatty acids liberated from VLDL triglycerides that are derived from liver. Tracing lipid fluxes under normal physiological conditions is technically very challenging, but the unique lipid paradigm revealed by the systemic lipid profiling in this study allowed us to model and examine lipid fluxes among key tissues. We first compared palmitoleate in FFA fractions and found that the concentrations of muscle palmitoleate closely resembled those observed in plasma, which were themselves a direct reflection of adipose FFAs (Figure 4A). In contrast, palmitoleate in muscle triglyceride showed a clear difference from the pattern of plasma TG palmitoleate, which was derived from liver (Figure 4A). These results suggest that the strong flux of palmitoleate from adipose tissue to muscle is the underlying mechanism for palmitoleate enrichment of this site in FABP$^{-/-}$ mice and is consistent with our previous projections. Consequently, palmitoleate levels were reduced in WT muscle by HFD. This reduction also occurred, but to a significantly less extent, in FABP$^{-/-}$ mice (Figure 4B), a pattern that matches the adipose tissue lipid profiles (Figure 2D). In light of palmitoleate's effect on improving insulin sensitivity in vitro, such a strong flux of this particular lipid from adipose tissue to muscle would have the potential to enhance insulin signaling at this site. We were unable to identify significant changes in neutral lipids and phospholipids (Figure S10), further supporting that the enrichment of palmitoleate is the major changes in muscle lipid metabolism of FABP$^{-/-}$ mice that might contribute to improved insulin sensitivity.

We next examined palmitoleate metabolism in WT and FABP$^{-/-}$ livers under conditions of regular and high-fat diet. Total palmitoleate was sharply increased by HFD in the liver tissue of WT but not in FABP$^{-/-}$ mice (Figure 4C), despite the fact that FABP$^{-/-}$ mice have dramatically increased plasma palmitoleate under both conditions. This result strongly suggests that the majority of palmitoleate in liver cannot be accounted for by adipose-derived FFAs. Indeed, palmitoleate levels in liver are closely associated with lipogenic gene expression at this site, consistent with endogenous production by hepatocytes. Several lipid synthetic genes, particularly SCD-1, were significantly increased by HFD in the liver tissues of WT but not FABP$^{-/-}$ mice (Maeda et al., 2005). Thus, the high levels of circulating palmitoleate in FABP$^{-/-}$ mice may play a regulatory role on the lipogenic programming of the liver rather than serve as a substrate to drive triglyceride synthesis. If this is indeed the case, reconstitution of SCD-1 should revert this phenotype. We expressed SCD-1 in the liver of FABP$^{-/-}$ mice on HFD using adenovirus-mediated gene expression in vivo (Figure S11).

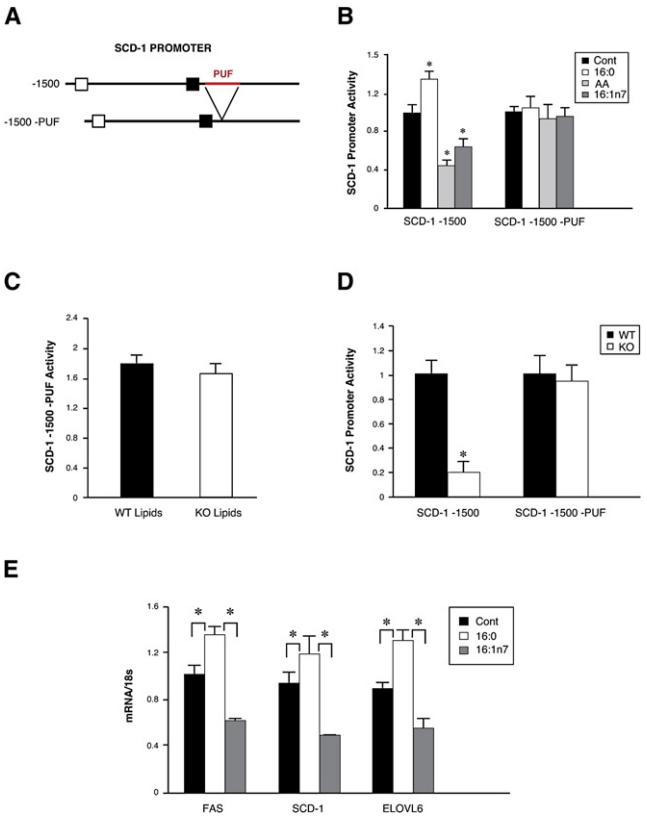


Figure 5. Lipid-Mediated Regulation of SCD-1 Promoter Activity In Vivo

(A) Schematics of SCD-1 −1500bp promoter. PUF, polyunsaturated fatty acid response element.

(B) Regulation of WT and mutant SCD-1 promoter activities by fatty acids. AA, arachidonic acid.

(C) Regulation of wild-type and mutant SCD-1 promoter activities by plasma lipids. Plasma lipids extracted from WT or FABP$^{-/-}$ (KO) mice were used to treat FAO cells infected with WT or mutant SCD-1 promoter-carrying adenoviruses, and luciferase assays were performed as described in the Experimental Procedures.

(D) In vivo regulation of WT and mutant SCD-1 promoter activities. Luciferase assays were performed on liver tissues of WT or KO mice injected with WT or mutant SCD-1 reporter-carrying adenoviruses.

(E) Liver gene expression in mice infused with vehicle, TG:palmitate or TG:palmitoleate. Asterisk, $p < 0.05$.

Error bars represent the SEM.

Expression of SCD-1 was sufficient to increase triglyceride synthesis in FABP$^{-/-}$ mice and elevated hepatic triglyceride levels similar to that of WT mice on HFD (Figure 4D). These data verify our hypothesis and demonstrates that suppression of SCD-1 activity is a key factor determining the liver steatosis phenotype in FABP$^{-/-}$ mice.

SCD-1 Expression Is Regulated by a Lipid Signal Derived from Adipose Tissue

To establish the link between lipid signals and FABP-deficiency-induced suppression of liver SCD-1, we designed a unique SCD-1 promoter-driven reporter system that had specifically lost its responsiveness to fatty acids. A short, 60 bp, polyunsaturated fatty acid response element (PUF) is required for regulation of SCD-1 expression by PUFA but not by hormones such as insulin (Waters et al., 1997) (Figure 5A). We deleted this PUF element from the SCD-1 promoter and produced adenoviruses to express this reporter. In FAO cells infected with the intact SCD-1 promoter reporter, transcriptional activity was suppressed by both AA and palmitoleate and increased by palmitate (Figure 5B). However, in cells expressing the mutant promoter, there was no difference in the reporter activity between control and lipid treatments (Figure 5B), demonstrating that the PUF element is specifically required for lipid regulation of the SCD-1 promoter. We then treated cells expressing the mutant promoter with WT or FABP$^{-/-}$ plasma lipid extracts. In this setting, the suppression of the SCD-1 promoter activity by FABP$^{-/-}$ lipids was lost (Figure 5C), demonstrating that the PUF sequence is required for the SCD-1 promoter to respond to plasma-derived lipids. To test this in mice, we injected the reporter adenoviruses into mice fed with HFD. The intact SCD-1 promoter was regulated in a manner similar to liver SCD-1 mRNA in vivo (Maeda et al., 2005), because promoter activity in the liver of WT mice was 5- to 10-fold higher than that observed in FABP$^{-/-}$ animals (Figure 5D). In contrast, activity of the mutant promoter showed no difference between FABP$^{-/-}$ mice and WT controls (Figure 5D). This result strongly suggests that reduced hepatic SCD-1 expression in FABP$^{-/-}$ mice is mediated by an adipose-derived plasma lipid signal, which is likely to be palmitoleate. To test this hypothesis, we studied the effects of lipid infusion on liver gene expression. After a 6 hr infusion as detailed in the next section, TG-palmitoleate caused a substantial decrease in SCD-1, fatty acid synthase (FAS), and fatty acid elongase 6 (ELOVL6) expression in liver compared to vehicle. In contrast, TG-palmitate infusion resulted in an increase in all of these lipogenic genes in liver (Figure 5E). These results confirm that the alteration of a single fatty acid in circulation can effectively regulate liver gene expression and that palmitoleate can indeed directly suppress SCD-1 expression in this in vivo setting.

Adipose-Specific Activation of De Novo Lipogenesis in the Absence of Lipid Chaperones

To investigate the molecular basis of altered de novo lipogenesis in FABP$^{-/-}$ mice, we examined lipogenic gene expressions in the adipose tissues of WT and FABP$^{-/-}$ mice. We detected marked stimulation (5- to 10-fold) of FAS, SCD-1, and ELOVL6, the three principal enzymes that mediate de novo fatty acid synthesis, in adipose tissues of FABP$^{-/-}$ mice (Figure 6A). This increase is remarkable considering that adipose tissue is already highly enriched in these enzymes. This gene expression profile is also in agreement with the increased concentration of palmitoleate, the main product of de novo lipogenesis. Interestingly, we also found that HFD significantly suppressed lipogenic gene expression in WT, but to a far lesser extent than in FABP$^{-/-}$ mice, which is consistent with reduced adipose tissue and plasma palmitoleate in WT but not in FABP$^{-/-}$ mice on a HFD.

The marked increase of genes involved in fatty acid synthesis in adipose tissue of FABP$^{-/-}$ mice and the unresponsiveness to HFD suggests that these lipid chaperones are integral components of lipid-mediated regulation of gene expression. To address this, we produced adipogenic cell lines from FABP$^{-/-}$

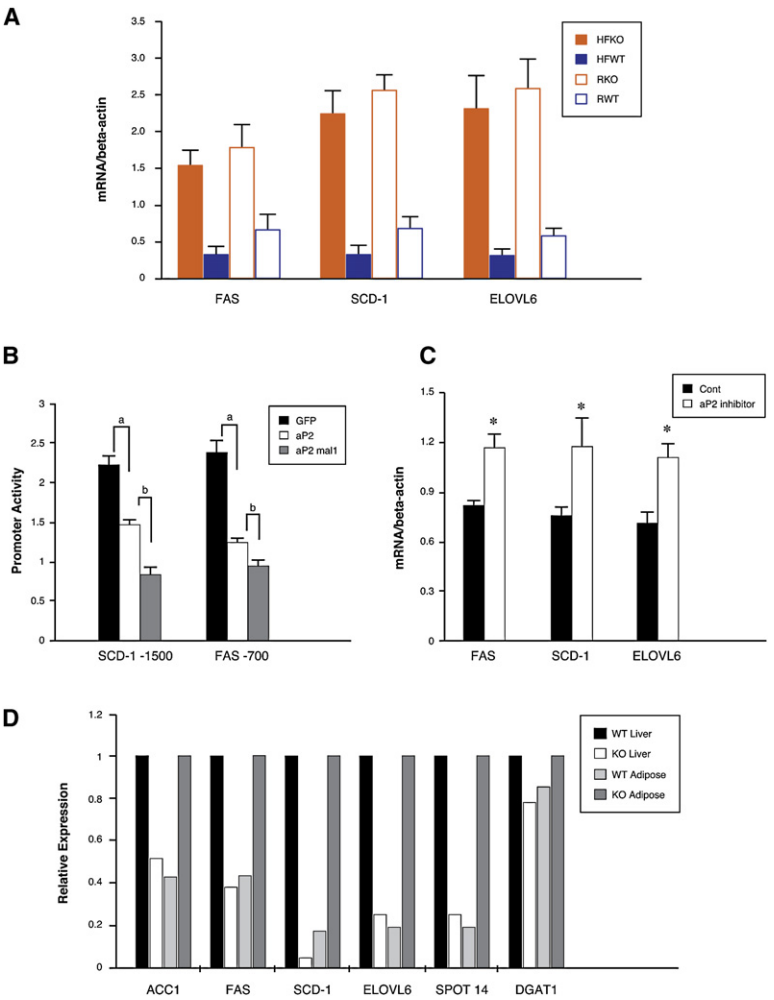


Figure 6. Regulation of Lipogenic Genes in Adipose and Liver of WT and FABP$^{-/-}$ Mice

(A) Lipogenic gene expression in adipose tissue of WT and FABP$^{-/-}$ (KO) mice. Gene expression patterns in epididymal fat pad were determined by quantitative real-time PCR.

(B) Regulation of lipogenic gene promoter activites by FABPs in differentiated adipocytes. Differentiated FABP$^{-/-}$ adipocytes that expressed SCD-1 or FAS promoter luciferase constructs were infected with GFP, aP2, or both aP2 and mal1 adenoviruses, and luciferase activities were determined by dual-glow luciferase system. a, significantly different from GFP-adenovirus-infected cells; b, significantly different from aP2-adenovirus-infected cells.

(C) Regulation of lipogenic gene expression in adipose tissue of mice treated with aP2 inhibitor. Gene expressions in epididymal fat pads from mice treated with vehicle or aP2 inhibitor were determined with quantitative real-time PCR.

(D) Differential regulation of lipogenic gene expression in adipose and liver tissues. Levels of the mRNAs in liver and epididymal fat pad from mice fed with HFD were determined, and WT liver and KO adipose were set as 1. ACC1, acetyl-CoA carboxylase1; DGAT1, acyl-CoA:diacylglycerol acyltransferase 1. Asterisk, $p < 0.05$.

Error bars represent the SEM.

mice and differentiated them into adipocytes (Figure S12). In this system, exogenously expressed FABPs strongly and additively suppressed both SCD-1 and FAS promoter activities (Figure 6B). These results indicate that lipid chaperones suppress the expression of lipogenic genes in adipocytes, and loss of these proteins leads to increased expression of genes in the lipid synthesis pathway, an observation consistent with our findings in the adipose tissue of FABP$^{-/-}$ mice. We also tested this pattern in vivo by blocking aP2 function in mice with an orally administrated synthetic inhibitor. This treatment generated effects that closely paralleled the beneficial phenotypes of genetic FABP deficiency (Furuhashi et al., 2007), and as would be expected, aP2 inhibitor treatment led to increased lipogenic gene expression in adipose tissues of WT mice (Figure 6C).

We have identified opposite patterns of SCD-1 expression in the liver versus adipose tissue of FABP$^{-/-}$ mice, a pattern likely regulated by the lipid palmitoleate. If our hypothesis were correct, this pattern would apply to other genes involved in lipogenesis in these tissues. Therefore, we extended our study to examine the major genes in fatty acid, cholesterol, and triglyceride synthesis. These genes also displayed a striking and diametrically opposite pattern of expression between adipose and liver tissues in WT and FABP$^{-/-}$ mice (Figure 6D).

Increased Circulating Palmitoleate Regulates Insulin Action

Intralipid infusion has been widely used to investigate the relationship between plasma FFAs and insulin resistance, but almost all studies using this protocol utilized preparations of natural lipid products containing a variety of fatty acids (Kim et al., 2004; Yu et al., 2002). To define the effects of individual fatty acids on metabolic regulation, we prepared Intralipid with triglycerides composed of a single fatty acid, either TG-palmitoleate or TG-palmitate. Infusion of either lipid resulted in a 2-fold increase in total plasma FFA levels with similar dynamics (Figure S13). Although TG-palmitate suppressed the entire proximal insulin-signaling pathway including activation of insulin receptor and phosphorylation of insulin receptor substrate 1, 2 and AKT in liver, TG-palmitoleate strongly potentiated these insulin actions (Figure 7A). We observed similar effects of both lipids on muscle tissue where palmitoleate enhanced and palmitate impaired insulin signaling (Figure 7B). These results clearly indicated that specific alteration of a single serum lipid is sufficient to regulate insulin action in peripheral tissues and that increased circulating palmitoleate enhances insulin sensitivity.

To investigate whether the increased insulin signaling by elevated serum palmitoleate can be translated into improved glucose metabolism, we performed hyperinsulinemic-euglycemic clamp studies on mice infused with either vehicle or palmitoleate. To enable delivery of the lipid at a rate that is compatible with clamp studies, we used fatty acid:palmitoleate instead of TG:palmitoleate and confirmed that palmitoleate enhanced muscle and liver insulin signaling in this setting by examining

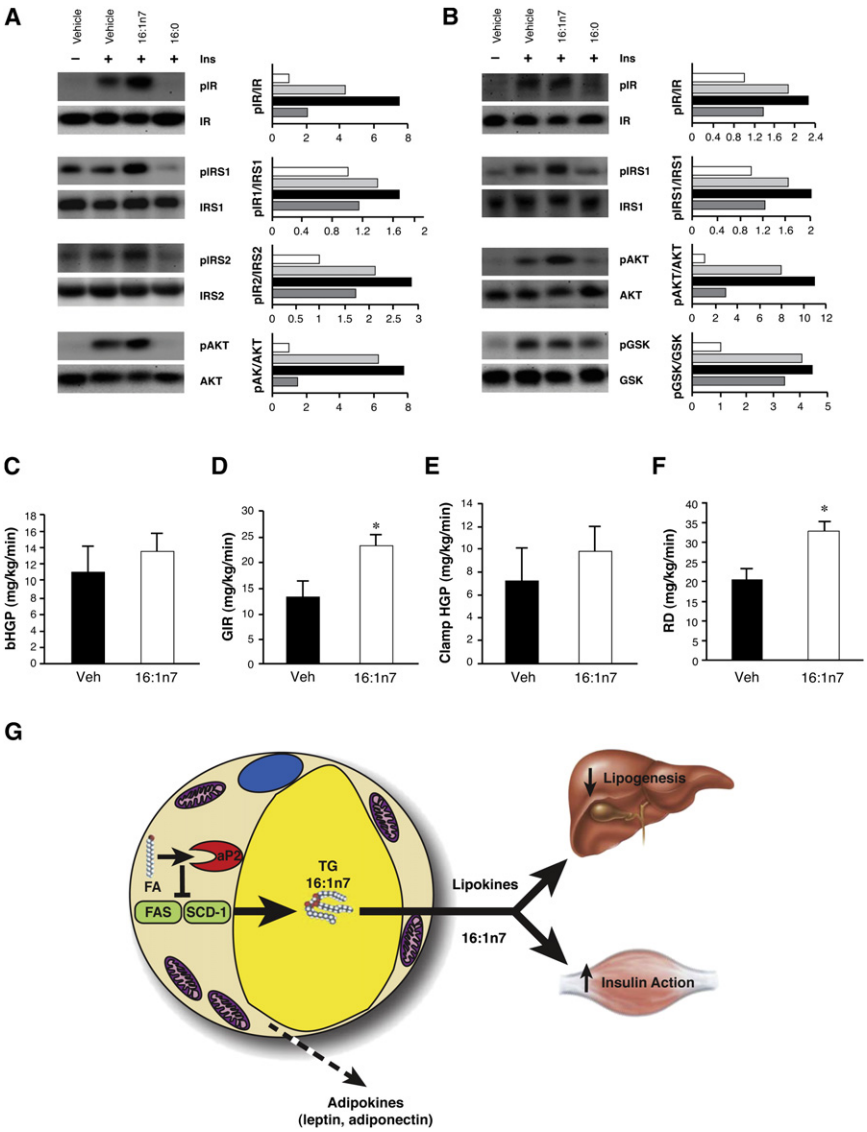


Figure 7. Regulation of Insulin Signaling and Glucose Metabolism by Palmitoleate

(A) Basal and insulin-stimulated phosphorylation of insulin receptor (IR), insulin receptor substrate-1 (IRS-1) and -2 (IRS-2), and AKT in liver of mice infused with vehicle (Veh), TG:palmitoleate (16:1n7), or TG:palmitate (16:0). Representative blots are shown, and quantifications on the right are averaged results of three mice in each treatment group.

(B) Basal and insulin-stimulated phosphorylation of insulin receptor (IR), insulin receptor substrate-1 (IRS-1), AKT, and GSK in muscle tissues of mice infused with vehicle (Veh), TG:palmitoleate (16:1n7) or TG:palmitate (16:0). Representative blots are shown, and quantifications on the right are averaged results of three mice in each treatment group.

(C) Basal hepatic glucose production (bHGP) of mice infused with vehicle (Veh) or palmitoleate (16:1n7).

(D) Glucose infusion rate (GIR) of mice treated with vehicle (Veh) or palmitoleate (16:1n7) during hyperinsulinemic-euglycemic clamp.

(E) Hepatic glucose production (Clamp HGP) of mice infused with vehicle (Veh) or palmitoleate (16:1n7) during hyperinsulinemic-euglycemic clamp.

(F) Glucose disposal rate (RD) in mice infused with vehicle (Veh) or palmitoleate (16:1n7) during hyperinsulinemic-euglycemic clamp.

(G) Regulation of systemic metabolic responses by adipose-derived lipid hormones (Lipokines). In parallel with a variety of adipokines, specific lipids released from adipocytes in response to physiological stimuli act at remote sites including liver and muscle and regulate systemic lipid and carbohydrate metabolism. Lipid chaperones negatively regulate one of these lipokines, C16:1n7-palmitoleate, and in the absence of these FABPs, strong flux of palmitoleate from adipose tissue to liver and muscle results in improved metabolic responses.

Error bars represent the SEM.

insulin stimulated activation of insulin receptor and AKT (Figure S14). Hyperinsulinemic-euglycemic clamp studies indicated that mice infused with palmitoleate required significantly higher glucose infusion rates to maintain euglycemia (Figure 7D). Neither basal nor clamped hepatic glucose production was significantly changed by palmitoleate infusion as compared to vehicle (Figures 7C and 7E). Instead, the increased glucose infusion rate in these mice was principally driven by enhanced whole-body glucose disposal (Figure 7F), confirming that the increased insulin signaling by palmitoleate can be directly reflected as improved glycemic control in conscious mice. These observations indicate that palmitoleate acts as an insulin-sensitizing hormone improving glucose metabolism.

DISCUSSION

Studies in recent years have identified adipose tissue as a critical site for whole-body metabolic regulation. Growing evidence supports the concept that peptides and hormones produced within adipose tissue constitute an important component of the endocrine effects of this site on systemic carbohydrate and lipid homeostasis. As the major storage site for lipids, adipose tissue has also been studied intensively in regards to its role in metabolic regulation through lipid signaling. Although equally critical as peptide hormones, this area has been more challenging to reduce into molecular entities and pathways. There are two prevailing views about the role of adipose tissue lipid metabolism in metabolic syndrome. First, storage of lipids in adipose tissue has been suggested to protect other organs from exposure to excessive lipids and thereby to reduce the risk of lipotoxicity. Second, fatty acids derived from adipose tissue, particularly under obese conditions, could disrupt the function of peripheral tissues, resulting in muscle insulin resistance or hepatic steatosis. In these models, the principal consideration has often been the total amount of lipid exposure at target tissues. However, serum lipids are very complex entities composed of structures with

varying chain length and saturation. The concentration and composition of fatty acids also vary significantly under different physiological and pathological conditions. Although it is unlikely that evaluation of total fatty acid levels alone is sufficiently informative, there has been little progress in addressing how different compositions of fatty acids in tissues or circulation affect the metabolic output, as this has been experimentally challenging. Another intractable question concerns how lipid-storing and/or -disposing tissues respond to dietary fatty acid intake and adjust their composition and hormonal output to modulate systemic metabolism.

In this report, we took advantage of high-resolution, quantitative lipidomic analysis combined with functional experimentation to approach these questions. We also utilized the striking impact of lipid chaperones on these paradigms in vivo to identify lipid pathways that contribute to systemic metabolic homeostasis. These approaches yielded several critical and unexpected results. First, we determined that the impact of diet on adipose lipid composition and metabolism is under strict control of adipose lipid chaperones and that these molecules ensure that dietary input is a dominant determinant of fatty acid composition in fat. In the absence of these proteins, adipose tissue is markedly refractory to the effects of diet on its lipid constituency and relies heavily on de novo lipogenesis. Second, we have demonstrated that adipose tissue regulates, in a lipid chaperone-dependent manner, the metabolic activities of distant organs through its lipid output and reduced this to a specific metabolic pathway in the liver. Third, we identified a unique fatty acid, palmitoleate, as a major signaling lipid hormone that controls several metabolic activities in liver and muscle tissues. Finally, these studies have allowed us to derive a model of the molecular mechanisms underlying the biology of lipid chaperones and how these molecules regulate an adipose-derived lipid hormone to generate their remarkable systemic effects.

How de novo lipogenesis in adipose tissue is affected by metabolic syndrome has remained an unresolved issue. Emerging evidence has suggested that adipose tissue has reduced lipid synthesis capacity in obese mice and human beings (Moraes et al., 2003; Nadler et al., 2000). Additionally, genetic or pharmacological manipulations that boost de novo lipogenesis in adipose tissue (even though this sometimes leads to expansion of the fat depot) are associated with improved metabolic homeostasis (Kuriyama et al., 2005; Waki et al., 2007), an outcome that is very different from that caused by dietary obesity (Kim et al., 2007; Watkins et al., 2002). One explanation for this is likely to be related to the differences in tissue and serum fatty acid profiles under the two obese conditions. The systemic approaches employed in our study demonstrated that in WT animals, consuming a HFD resulted in increased lipid content of adipose tissue, and the composition of this tissue did not differ from those of muscle or liver as the same lipids contributed to the systemic circulation. In contrast, enhanced de novo lipogenesis in adipose tissue, which occurs in the absence of lipid chaperons, actively alters tissue and serum fatty acids, particularly palmitoleate, contributing to improved metabolic homeostasis regardless of the total lipid mass.

Our results also raise the possibility that palmitoleate is a major signaling lipid produced from adipose tissue. Several properties of this particular fatty acid fit well into a regulatory role as an adipose tissue-derived hormone. For example, even though fatty acids of all chain lengths and saturation are produced as intermediate products, only palmitoleate is significantly and abundantly accumulated by elevated de novo lipogenesis in adipose tissue. This is potentially due to enzymatic specificity of FAS and coordinated regulation of SCD-1. As a result, palmitoleate might be the only fatty acid that could substantially change serum fatty acid composition in relation to alterations in lipid metabolism in adipose tissue. Unlike its saturated counterpart palmitate, which is already highly enriched in the sn-1 position of phospholipids and triglycerides and is resistant to further enrichment, newly synthesized palmitoleate can be efficiently incorporated into different lipid classes and dramatically alter its enrichment in a variety of compartments. The low basal levels and rapid fluctuations reflecting de novo lipogenesis again support the notion that palmitoleate is suitable to serve as a regulatory signal or a hormone. This characteristic also distinguishes palmitoleate from oleate, which is very abundant in most tissues and rarely exhibits substantial concentration changes under normal physiological conditions. Hence, palmitoleate has the capacity to serve as a lipid signal that mediates communications between adipose and other tissues, and we suggest that it be considered a ''lipokine'' (Figure 7G).

The highly coordinated regulation of lipid flux and metabolism suggests that adipose-specific activation of de novo lipogenesis might lead to a beneficial general metabolic profile through its systemic effects. If the increased products of lipogenesis in adipose tissue can efficiently suppress liver lipid production, the net outcome of adipose-specific activation of de novo lipogenesis would be anticipated to be decreased total body weight with improved metabolic profiles. This scenario is in contrast to enhanced lipogenesis in liver, which often increases overall adiposity even though both conditions could have elevated serum palmitoleate (Paillard et al., 2007). This adipose-controlled lipid profile is observed in FABP$^{-/-}$ mice, which exhibit markedly increased palmitoleate in blood and striking protection against metabolic disease along with the benefits of SCD-1 activation in the adipose tissue to convert toxic saturated fatty acids to unsaturated ones. If similar patterns could be extrapolated to humans, compositional studies might offer new biomarkers to monitor disease susceptibility, guide preventive strategies, and even lead to clinical interventions with naturally occurring lipid products (Hiraoka-Yamamoto et al., 2004).

EXPERIMENTAL PROCEDURES

Animals

Mice with homozygous null mutations in *aP2* and *mal1* were backcrossed more than 12 generations into C57BL/6J genetic background as previously described (Maeda et al., 2005). WT littermates were used as controls. Mice were maintained on regular chow diet (RD) or placed on HFD at 4 weeks of age for 16 weeks to induce dietary obesity. WT Mice on HFD diet were administered with aP2 inhibitor daily via oral gavage at a dose of 40 mg/kg/day for 2 months. Adipose tissues were collected at the end of the treatment for gene expression analyses. The Harvard Medical Area Standing Committee on Animals approved all studies.

Quantitative Lipid Profiling

Lipids from plasma and tissues were extracted in the presence of authentic internal standards by the method of Folch et al. (1957) with chloroform:methanol (2:1 v/v). Individual lipid classes were separated by liquid chromatography

(Agilent Technologies model 1100 Series). Each lipid class was transesterified in 1% sulfuric acid in methanol under a nitrogen atmosphere at 100°C for 45 min. The resulting fatty acid methyl esters were extracted from the mixture with hexane containing 0.05% butylated hydroxytoluene and prepared for gas chromatography under nitrogen. Fatty acid methyl esters were separated and quantified by capillary gas chromatography (Agilent Technologies model 6890) equipped with a 30 m DB-88MS capillary column (Agilent Technologies) and a flame-ionization detector.

Adenovirus Production and Infection of Adipocytes and Mouse

Expression and luciferase reporter adenoviruses were constructed as described in the Supplemental Data. Five microliters crude virus was used to infect differentiated adipocytes in 96-well plate for reporter assays. Adenoviruses used to infect mice were purified with CsCl ultracentrifugation and desalted with a PD 10 column. Adenoviruses were tittered and administrated via tail vein injection (10^{11} viral particles per mouse).

Plasma Lipid Extraction, Lipid Treatments, Immunoprecipitation, and Immunoblotting

Two hundred microliters serum was collected and spun at 13,000 g in a microcentrifuge to separate the plasma. Plasma lipids were extracted by the addition of 0.3 ml 0.5 M KH_2PO_4, 1.5 ml chloroform, and 0.5 ml methanol. After vortexing 2 min and centrifugation, the lower phase was collected and evaporated. Lipids were dissolved in 50 μl DMEM with 2% fatty acid-free BSA. Two microliters of either whole plasma or plasma lipids was used to treat cells in 96-well plates. Tissue protein lysates was separated with SDS-PAGE gels and phosphorylated, or total proteins were detected with the following antibodies: phospho-AKT Serine 473, AKT, insulin receptor, and phospho-tyrosine from Santa Cruz Biotechnology; IRS-1 and IRS-2 from Upstate; phospho-GSK and GSK from Cell Signaling Technology; and phospho-insulin receptor from Calbiochem. For the immunoprecipitation of IRS-1 and IRS-2, 1000 μg tissue protein lysate was incubated with 3 μl anti-IRS-1 or -2 antibodies and 40 μl Protein A beads (Amersham) overnight. Proteins bound to beads were eluted with SDS loading buffer.

Lipid Infusion and Hyperinsulinemic-Euglycemic Clamp

Intralipid solution with 2 mM triglycerides:palmitate or palmitoleate was prepared via a previously described protocol with modifications (Stein et al., 1997). In brief, lipids were dissolved in a solvent containing 5% glycerol and 0.72% phosphocholine in 0.9% saline, heated at 80°C for 10 min, and sonicated repeatedly. For TG:palmitoleate, the heating was omitted to avoid oxidization of the lipids. Lipids will stay in suspension for 1 week and need to be vortexed well before loading of the syringe and tubing to prevent clogging. Seven days before lipid infusion, mice were anesthetized, and an indwelling catheter was inserted in the left internal jugular vein. After overnight fasting, lipids were infused at a rate of 500 μl/kg/min for 6 hr. At the end of the infusion, insulin (1 U/Kg) was injected into mice via the infusion tubing, and tissues were collected. For the determination of serum FFA level during lipid infusion, blood was collected from mouse tails at different time intervals and spun down for the collection of plasma. Serum FFAs were determined with a commercial kit (Wako Chemicals). TG:palmitate and TG:palmitoleate are difficult to dissolve at concentrations that are compatible with the infusion rate of hyperinsulinemic-euglycemic clamp study while maintaining efficient delivery of these lipids. Therefore, fatty acid:palmitoleate was used for the infusion of mice for clamp study. Palmitoleate was dissolved in saline containing 2% BSA (vehichle) at 15 mM with repeated sonications and was infused through the tubing at a rate of 3.3 μl/min for 2 hr. A standard hyperinsulinemic-euglycemic clamp was performed (Furuhashi et al., 2007). Vehicle or palmitoleate solution was used to dissolve tracer ^{3}H-glucose so lipid was also infused at 3.3 μl /min throughout the 4 hr period of clamp study.

SUPPLEMENTAL DATA

Supplemental Data include Supplemental Experimental Procedures and 15 figures and can be found with this article online at http://www.cell.com/cgi/content/full/134/6/933/DC1/.

ACKNOWLEDGMENTS

We thank Deniz Hotamisligil for artistic rendition and design input. We gratefully acknowledge the assistance of Harold Emsheimer and UyenThao Nguyen (Lipomics Technologies) for their help with composing the figures and performing statistic analyses, respectively. We are grateful to the members of the Hotamisligil Lab for their input and contributions, especially Masato Furuhashi for his help with the hyperinsulinemic-euglycemic clamp studies and Rebecca Foote for administrative support. This work was supported by a National Institutes of Health (NIH) grant DK064360 (to G.S.H.), and H.C. is supported by a NIH roadmap fellowship (DK71507-04) and the American Diabetes Association. M.M.W. and S.M.W. are employees of Lipomics Technologies (West Sacramento, CA). G.S.H. serves as a member of the scientific advisory board at Lipomics Technologies.

Received: December 18, 2007
Revised: June 5, 2008
Accepted: July 22, 2008
Published: September 18, 2008

REFERENCES

Avramoglu, R.K., Basciano, H., and Adeli, K. (2006). Lipid and lipoprotein dysregulation in insulin resistant states. Clin. Chim. Acta *368*, 1–19.

Bergman, R.N., and Ader, M. (2000). Free fatty acids and pathogenesis of type 2 diabetes mellitus. Trends Endocrinol. Metab. *11*, 351–356.

Cao, H., Maeda, K., Gorgun, C.Z., Kim, H.J., Park, S.Y., Shulman, G.I., Kim, J.K., and Hotamisligil, G.S. (2006). Regulation of metabolic responses by adipocyte/macrophage Fatty Acid-binding proteins in leptin-deficient mice. Diabetes *55*, 1915–1922.

Chu, K., Miyazaki, M., Man, W.C., and Ntambi, J.M. (2006). Stearoyl-coenzyme A desaturase 1 deficiency protects against hypertriglyceridemia and increases plasma high-density lipoprotein cholesterol induced by liver X receptor activation. Mol. Cell. Biol. *26*, 6786–6798.

Eckel, R.H., Grundy, S.M., and Zimmet, P.Z. (2005). The metabolic syndrome. Lancet *365*, 1415–1428.

Field, C.J., and Clandinin, M.T. (1984). Modulation of adipose tissue fat composition by diet: A review. Nutr. Res. *4*, 743–755.

Folch, J., Lees, M., and Sloane Stanley, G.H. (1957). A simple method for the isolation and purification of total lipides from animal tissues. J. Biol. Chem. *226*, 497–509.

Furuhashi, M., and Hotamisligil, G.S. (2008). Fatty acid-binding proteins: Role in metabolic diseases and potential as drug targets. Nat. Rev. Drug Discov. *7*, 489–503.

Furuhashi, M., Tuncman, G., Gorgun, C.Z., Makowski, L., Atsumi, G., Vaillancourt, E., Kono, K., Babaev, V.R., Fazio, S., Linton, M.F., et al. (2007). Treatment of diabetes and atherosclerosis by inhibiting fatty-acid-binding protein aP2. Nature *447*, 959–965.

Ginsberg, H.N., Zhang, Y.L., and Hernandez-Ono, A. (2006). Metabolic syndrome: Focus on dyslipidemia. Obesity (Silver Spring) *14* (*Suppl 1*), 41S–49S.

Heinemann, F.S., and Ozols, J. (2003). Stearoyl-CoA desaturase, a short-lived protein of endoplasmic reticulum with multiple control mechanisms. Prostaglandins Leukot. Essent. Fatty Acids *68*, 123–133.

Hiraoka-Yamamoto, J., Ikeda, K., Negishi, H., Mori, M., Hirose, A., Sawada, S., Onobayashi, Y., Kitamori, K., Kitano, S., Tashiro, M., et al. (2004). Serum lipid effects of a monounsaturated (palmitoleic) Fatty Acid-rich diet based on macadamia nuts in healthy, young Japanese women. Clin. Exp. Pharmacol. Physiol. *31* (*Suppl 2*), S37–S38.

Hotamisligil, G.S. (2006). Inflammation and metabolic disorders. Nature *444*, 860–867.

Hotamisligil, G.S., Johnson, R.S., Distel, R.J., Ellis, R., Papaioannou, V.E., and Spiegelman, B.M. (1996). Uncoupling of obesity from insulin resistance through a targeted mutation in aP2, the adipocyte fatty acid binding protein. Science *274*, 1377–1379.

Kim, J.K., Fillmore, J.J., Sunshine, M.J., Albrecht, B., Higashimori, T., Kim, D.W., Liu, Z.X., Soos, T.J., Cline, G.W., O'Brien, W.R., et al. (2004). PKC-theta knockout mice are protected from fat-induced insulin resistance. J. Clin. Invest. *114*, 823–827.

Kim, J.Y., van de Wall, E., Laplante, M., Azzara, A., Trujillo, M.E., Hofmann, S.M., Schraw, T., Durand, J.L., Li, H., Li, G., et al. (2007). Obesity-associated improvements in metabolic profile through expansion of adipose tissue. J. Clin. Invest. *117*, 2621–2637.

Kuriyama, H., Liang, G., Engelking, L.J., Horton, J.D., Goldstein, J.L., and Brown, M.S. (2005). Compensatory increase in fatty acid synthesis in adipose tissue of mice with conditional deficiency of SCAP in liver. Cell Metab. *1*, 41–51.

Maeda, K., Cao, H., Kono, K., Gorgun, C.Z., Furuhashi, M., Uysal, K.T., Cao, Q., Atsumi, G., Malone, H., Krishnan, B., et al. (2005). Adipocyte/macrophage fatty acid binding proteins control integrated metabolic responses in obesity and diabetes. Cell Metab. *1*, 107–119.

Moraes, R.C., Blondet, A., Birkenkamp-Demtroeder, K., Tirard, J., Orntoft, T.F., Gertler, A., Durand, P., Naville, D., and Begeot, M. (2003). Study of the alteration of gene expression in adipose tissue of diet-induced obese mice by microarray and reverse transcription-polymerase chain reaction analyses. Endocrinology *144*, 4773–4782.

Nadler, S.T., Stoehr, J.P., Schueler, K.L., Tanimoto, G., Yandell, B.S., and Attie, A.D. (2000). The expression of adipogenic genes is decreased in obesity and diabetes mellitus. Proc. Natl. Acad. Sci. USA *97*, 11371–11376.

Newberry, E.P., Xie, Y., Kennedy, S.M., Luo, J., and Davidson, N.O. (2006). Protection against Western diet-induced obesity and hepatic steatosis in liver fatty acid-binding protein knockout mice. Hepatology *44*, 1191–1205.

Ntambi, J.M. (1999). Regulation of stearoyl-CoA desaturase by polyunsaturated fatty acids and cholesterol. J. Lipid Res. *40*, 1549–1558.

Ntambi, J.M., and Miyazaki, M. (2004). Regulation of stearoyl-CoA desaturases and role in metabolism. Prog. Lipid Res. *43*, 91–104.

Paillard, F., Catheline, D., Duff, F.L., Bouriel, M., Deugnier, Y., Pouchard, M., Daubert, J.C., and Legrand, P. (2007). Plasma palmitoleic acid, a product of stearoyl-coA desaturase activity, is an independent marker of triglyceridemia and abdominal adiposity. Nutr. Metab. Cardiovasc. Dis. *18*, 436–440.

Stein, D.T., Stevenson, B.E., Chester, M.W., Basit, M., Daniels, M.B., Turley, S.D., and McGarry, J.D. (1997). The insulinotropic potency of fatty acids is influenced profoundly by their chain length and degree of saturation. J. Clin. Invest. *100*, 398–403.

Tuncman, G., Erbay, E., Hom, X., De Vivo, I., Campos, H., Rimm, E.B., and Hotamisligil, G.S. (2006). A genetic variant at the fatty acid-binding protein aP2 locus reduces the risk for hypertriglyceridemia, type 2 diabetes, and cardiovascular disease. Proc. Natl. Acad. Sci. USA *103*, 6970–6975.

Waki, H., Park, K.W., Mitro, N., Pei, L., Damoiseaux, R., Wilpitz, D.C., Reue, K., Saez, E., and Tontonoz, P. (2007). The small molecule harmine is an antidiabetic cell-type-specific regulator of PPARgamma expression. Cell Metab. *5*, 357–370.

Warensjo, E., Riserus, U., and Vessby, B. (2005). Fatty acid composition of serum lipids predicts the development of the metabolic syndrome in men. Diabetologia *48*, 1999–2005.

Waters, K.M., Miller, C.W., and Ntambi, J.M. (1997). Localization of a polyunsaturated fatty acid response region in stearoyl-CoA desaturase gene 1. Biochim. Biophys. Acta *1349*, 33–42.

Watkins, S.M., Reifsnyder, P.R., Pan, H.J., German, J.B., and Leiter, E.H. (2002). Lipid metabolome-wide effects of the PPARgamma agonist rosiglitazone. J. Lipid Res. *43*, 1809–1817.

Yu, C., Chen, Y., Cline, G.W., Zhang, D., Zong, H., Wang, Y., Bergeron, R., Kim, J.K., Cushman, S.W., Cooney, G.J., et al. (2002). Mechanism by which fatty acids inhibit insulin activation of insulin receptor substrate-1 (IRS-1)-associated phosphatidylinositol 3-kinase activity in muscle. J. Biol. Chem. *277*, 50230–50236.